

A HEURISTIC ALGORITHM FOR PARAMETER IDENTIFICATION OF STEEL MATERIALS UNDER ASYMMETRIC CYCLIC ELASTOPLASTIC DEFORMATION

Makoto Ohsaki ^{1*}, Jingyao Zhang ², Tomoshi Miyamura ³

¹*Dept. of Architecture, Hiroshima University, Higashi-Hiroshima 739-8527, Japan, ohsaki@hiroshima-u.ac.jp*

²*Dept. of Architecture and Urban Design, Nagoya City University, Nagoya 464-0083, Japan, zhang@sda.nagoya-cu.ac.jp*

³*Dept. of Computer Science, Nihon University, Koriyama 963-8642, Japan, miyamura@cs.ce.nihon-u.ac.jp*

Abstract

An optimization approach is presented for parameter identification of a constitutive model of steel materials. The variables are the yield stress, the hardening coefficients, and the ratio of isotropic hardening to the total hardening including kinematic hardening. The objective function to be minimized is the error between the stresses of experimental and numerical results under specified cyclic deformation. We discretize the variables into integer values, and formulate the problem as a combinatorial optimization problem. Some tools of statistical analysis and data mining are used to improve accuracy of solution. The hardening coefficients for specific structural experiments are identified from the monotonic uniaxial tests using a heuristic approach called tabu search. It is shown that the relation between the bending moment and the average deflection angle can be successfully simulated for symmetric, asymmetric, and random loading protocols.

Keywords: *Steel material, Parameter identification, Statistical analysis, Random selection, Decision tree*

1. Introduction

In the fields of mechanical engineering and material science, various constitutive models, including Armstrong-Frederic model, multi-layer model, and bounding surface model, have been developed for simulating cyclic elastoplastic behavior of steel materials [1]. In contrast, one of the important and distinct properties of rolled mild steel materials used in civil and architectural engineering is the existence of a sharp yield plateau at the first yielding [2].

The Bauschinger effect should also be incorporated to simulate different characteristics between the first and subsequent loadings. We developed a semi-implicit model based on explicit evaluational rule using the von Mises yield condition and implicit and heuristic rule of a piecewise-linear combined isotropic-kinematic hardening [3]. Different rules are used for the first and subsequent loading states.

In this study, we present an optimization approach to parameter identification of the constitutive model of rolled mild steel materials. The variables are the yield stress, hardening coefficients, and the ratio of isotropic hardening to the total hardening including kinematic hardening. The objective function to be minimized is the error between the stresses of experimental and numerical results under specified cyclic deformation. Since the optimization problem is highly nonlinear, we discretize the variables into integer values, and formulate the problem as a combinatorial optimization problem. Another difficulty in parameter identification is that the feasible regions of parameters are very difficult to assign without any *a priori* knowledge. Furthermore, the redundancy of material parameters becomes significant if the accuracy of the stress-strain relation is to be improved uniformly throughout the cyclic process; i.e., there are many different solutions that have approximately the same objective value as the optimal solution. In order to overcome these difficulties, we employ some techniques of data mining and statistical analysis. The effectiveness of the proposed method is demonstrated through simulation of cyclic material test, and structural test results of cantilever subjected to cyclic deformation.

2. Constitutive model of steel material

Consider a steel material model based on von Mises yield criterion and linear hardening. Let $\bar{\epsilon}^p$ denote the equivalent plastic strain. The hardening coefficient $h(\bar{\epsilon}^p)$ is divided into two parts of kinematic hardening and isotropic hardening as

$$h(\bar{\epsilon}^p) = c_K h(\bar{\epsilon}^p) + c_I h(\bar{\epsilon}^p) \quad (1)$$

where c_K and c_I , satisfying $c_K + c_I = 1$, are the parameters for defining the ratios of kinematic hardening and isotropic hardening, respectively. We define $h(\bar{\epsilon}^p)$ as a piecewise-linear function of $\bar{\epsilon}^p$.

In order to model the yield plateau at the first plastic loading, different functions are assigned for $h(\bar{\epsilon}^p)$ for the first and subsequent loadings. The increment from re-loading point is used for $\bar{\epsilon}^p$ of the subsequent loading. Furthermore, a small

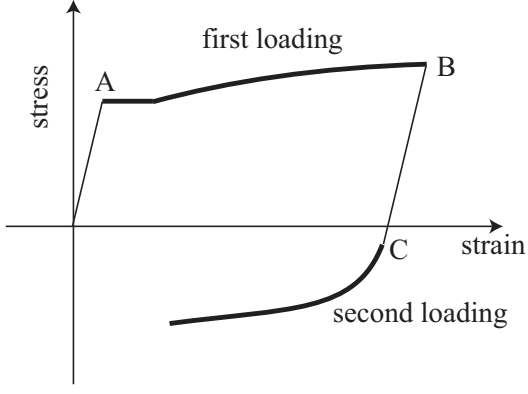


Figure 1: Stress-strain relation for first and second loadings.

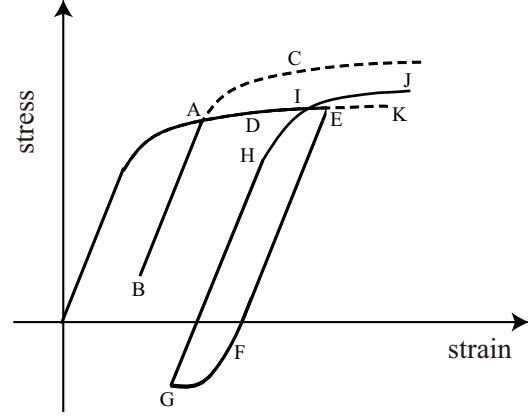


Figure 2: Hardening properties at re-loading.

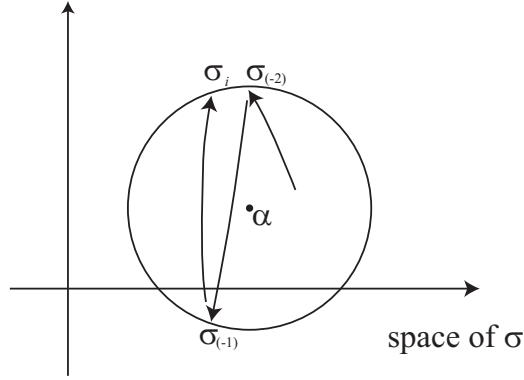


Figure 3: Re-loading in a process of asymmetric cyclic loading.

interval with negative ratio $c_1^{(1)}$ of isotropic hardening is assigned after the first yielding, because the difference of stresses at the unloading point B and the re-loading point C in Fig. 1 is smaller than the twice of yield stress.

Let $\hat{\sigma}$ denote the equivalent stress. The maximum value of $\hat{\sigma}$ experienced so far is denoted by $\hat{\sigma}^{\max}$. The size of yield surface increases with the cyclic deformation if $\hat{\sigma}$ is greater than $\hat{\sigma}^{\max}$; otherwise, the stress-strain relation exhibits a loop of constant size. Therefore, the different values $c_1^{(2)}$ and $c_1^{(3)}$ are used for the cases $\hat{\sigma} < \hat{\sigma}^{\max}$ and $\hat{\sigma} \geq \hat{\sigma}^{\max}$, respectively, for subsequent loadings.

In the process of uniaxial cyclic loading as shown in Fig. 2, the stress-strain relation follows the previous curve ADEK after unloading at 'A' and direction reversal at 'B' after elastic deformation. In contrast, the stress-strain relation follows a different curve HIJ after unloading at 'E', loading at 'F', and unloading at 'G'. In order to model this property, stresses at the previous and the second previous unloading point are recorded as $\sigma_{(-1)}$ and $\sigma_{(-2)}$, respectively, as shown in Fig. 3. The stress-strain relation follows the original curve, if the norm of $\sigma_{(-1)} - \sigma_{(-2)}$ is smaller than the specified value, or the reloading occurs without loading in the opposite direction.

3. Parameter identification

3.1 Formulation of optimization problem

The parameters are identified using the cyclic material test results in [6]. Young's modulus is identified from the initial elastic stiffness. The hardening coefficients in the initial (curve 1) and subsequent (curve 2) loadings are denoted by subscripts 1 and 2, respectively, and the same value is given for the cases $\hat{\sigma} < \hat{\sigma}^{\max}$ and $\hat{\sigma} \geq \hat{\sigma}^{\max}$ in curve 2. The values in the i th interval of \bar{e}^p in each curve are denoted by the superscript $[i]$. A small value is given for $h_1^{[2]}$ on the yield plateau, as well as the threshold values classifying curves 2 and 3.

Let $\tilde{\sigma}(t_i)$ and $\tilde{\epsilon}(t_i)$ denote the stress and strain at time t_i of the i th step of pseudo-static cyclic test. The stress simulated by cyclic analysis in the same condition as the experiment is denoted as $\hat{\sigma}^a(t_i)$. Then the objective function is defined as

$$\tilde{E}(X) = \sqrt{\frac{1}{|\mathcal{P}|} \sum_{i \in \mathcal{P}} [\hat{\sigma}^a(t_i) - \tilde{\sigma}(t_i)]^2} \quad (2)$$

Table 1: Upper and lower bounds of variables.

	lower bound	upper bound (Step 1)	updated upper bound (Steps 2, 3, 4)
$X_1 = c_1^{(1)}$	-20.0	-10.0	-10.0
$X_2 = c_1^{(2)}$	0.0	0.02	0.02
$X_3 = c_1^{(3)}$	0.3	0.8	0.67
$X_4 = h_1^{[1]}$	80000.0	180000.0	180000.0
$X_5 = h_2^{[1]}$	20000.0	120000.0	110000.0
$X_6 = h_2^{[2]}$	10000.0	80000.0	45000.0
$X_7 = h_2^{[3]}$	5000.0	10000.0	10000.0
$X_8 = h_2^{[4]}$	1000.0	8000.0	8000.0
$X_9 = h_2^{[5]}$	100.0	5000.0	5000.0
$X_{10} = h_2^{[6]}$	100.0	5000.0	4500.0
$X_{11} = h_2^{[7]}$	100.0	5000.0	3800.0
$X_{12} = \sigma_y^0$	260.0	270.0	270.0

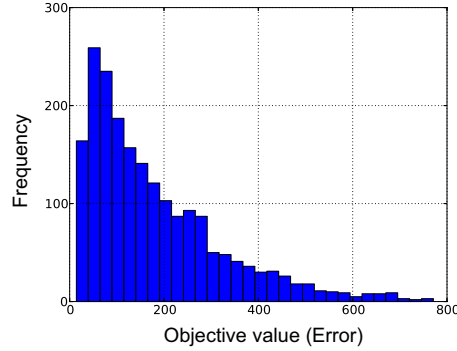


Figure 4: Histogram of objective function $E(\mathbf{J})$ (Step 1).

where $\mathbf{X} = (X_1, \dots, X_m)$ is the vector of m variables consisting of hardening coefficients, the ratios of isotropic hardening, and the yield stress σ_y^0 . Note that the error is evaluated only in the plastic loading state denoted by \mathcal{P} .

Let n_2 denote the number of intervals in curve 2. The following constraints are given so that the hardening coefficient is a non-increasing function of the equivalent plastic strain.

$$h_2^{[i]} \geq h_2^{[i+1]}, \quad (i = 1, \dots, n_2 - 1) \quad (3)$$

In the following results, the units of length and force are mm and N, respectively, which are omitted for brevity. Since the objective function is a highly nonlinear function of the variables, the variables are discretized and represented, as follows, by s integer values $J_i \in \{1, \dots, s\}$ ($i = 1, \dots, m$) with the upper and lower bounds X_i^U and X_i^L for X_i , as shown in Table 1:

$$X_i = X_i^L + \frac{J_i - 1}{s - 1} (X_i^U - X_i^L), \quad (i = 1, \dots, m) \quad (4)$$

Therefore, all properties are functions of \mathbf{J} , and the objective function is denoted by $E(\mathbf{J})$.

3.2 Result of parameter identification

The 12 variables defined in Table 1 are sampled to 20 values, i.e., $s = 20$, and random selection is carried out 2000 times with replacement. The range of objective functions by 2000 selections is [14.22, 771.16]. This process is called Step 1, and its distribution of objective value is shown in Fig. 4.

The probability $P(a)$ such that one of the best $a\%$ solutions cannot be obtained after 2000 random selection is $(1 - 0.01a)^{2000}$; i.e., $P(1) = 1.86 \times 10^{-9}$, $P(0.5) = 4.43 \times 10^{-5}$, and $P(0.1) = 0.1352$. Therefore, the probability of obtaining a best 0.5% solution is more than 99.99%. However, the number of 0.5% solutions is 2.048×10^{13} out of the total $20^{12} = 4.096 \times 10^{15}$ solutions. If we assume the objective value is uniformly distributed, the error in the objective value is 3.785, which is equal to 0.5% of the range [14.22, 771.16]. Since the distribution is non-uniform and has large

Table 2: Optimal solutions of four steps.

	Step 1	Step 2	Step 3	Step 4
$X_1 = c_1^{(1)}$	-12.105	-14.737	-17.89	-17.89
$X_2 = c_1^{(2)}$	0.00211	0.00211	0.00316	0.00316
$X_3 = c_1^{(3)}$	0.58947	0.65053	0.63105	0.63105
$X_4 = h_1^{[1]}$	180000	169470	143160	143160
$X_5 = h_2^{[1]}$	41053	62632	45000	45000
$X_6 = h_2^{[2]}$	32105	45000	45000	45000
$X_7 = h_2^{[3]}$	9210.5	5526.3	8947.4	8947.4
$X_8 = h_2^{[4]}$	6894.7	2047.4	5052.6	5052.6
$X_9 = h_2^{[5]}$	2678.9	2047.4	3039.5	3039.5
$X_{10} = h_2^{[6]}$	1389.5	2047.4	1026.3	1026.3
$X_{11} = h_2^{[7]}$	615.79	2047.4	878.95	878.95
$X_{12} = \sigma_y^0$	267.37	264.21	264.21	264.21
Error	14.217	14.117	12.082	12.082

density in the region of small objective value, as shown in Fig. 4, we can have conservative estimate by assuming uniform distribution. The best solution is listed in the first column of Table 2.

In the following, the 100 best solutions out of 2000 solutions are regarded as decent solutions, or approximate optimal solutions, where the objective value of the 100th solution is 34.6366. The properties of decent solutions are investigated to improve the accuracy of solutions. The first row of Table 3 (Step 1) shows the mean value and standard variation of each integer variable in decent solutions, which shows that standard deviation is very large.

In order to clarify redundancy of variables, which leads to large deviation of decent solutions, the contribution of each variable on objective value is investigated using the χ -square test of goodness of fit. A data mining tool called WEKA Ver. 3.6 [7, 8] is used for this purpose. The decent solutions and other solutions are categorized as ‘SMALL’ and ‘LARGE’, respectively.

By carrying out ‘ChiSquareAttributeEval’ without cross-validation, we obtain the following output:

```

Ranked attributes:
88.583  6  J6
45.731  3  J3
31.609  5  J5
24.397 11  J11
23.913 10  J10
21.634  2  J2
10.453  4  J4
0       1  J1
0       8  J8
0       9  J9
0      12  J12
0       7  J7

```

Since the number of categories is 2, the χ^2 -distribution of freedom 1 is to be used, and $\chi_{0.05}^2(1) = 7.879$. Therefore, the objective function is not independent of $J_6, J_3, J_5, J_{11}, J_{10}, J_2$, and J_4 with confidence 5%. Multiple linear regression of objective function is also carried out for 2000 solutions as shown in Table 4. As is seen, all P-values of J_9 and J_{12} are very large; therefore, these variables have small effect on the objective function. This is because the feasible region [260, 270] for J_{12} is small enough, and the values of J_6, \dots, J_{12} are adjusted so that Eq. (3) is satisfied. We can confirm also from Table 4 that the objective value strongly depends on J_3 and J_6 , because their coefficients are very large.

We next use a machine learning algorithm called ‘alternating decision tree’ (ADTree) to identify properties of variables to search smaller feasible region. Standard approaches of decision tree, such as J48, which is a Java implementation of C.45, are also available in WEKA. However, the output of J48 is difficult to interpret. In contrast, the result of ADTree is described by contribution score at each node, which is to be summed to the leaf to find the total contribution. Using the tool implemented in WEKA, we obtain the results in Fig. 5.

We can see from this result that 95% of the solutions is correctly classified to SMALL or LARGE. The number

Table 3: Mean value and standard deviation of decent solutions sampled to integer values.

		J_1	J_2	J_3	J_4	J_5	J_6	J_7	J_8	J_9	J_{10}	J_{11}	J_{12}
Step 1	mean	9.70	8.95	6.66	11.25	8.61	5.93	10.45	9.39	9.79	8.12	8.23	9.49
	std. dev.	5.72	5.11	4.24	5.51	4.57	3.61	6.05	5.78	5.48	4.67	4.34	5.99
Step 2	mean	11.37	7.48	10.47	11.37	9.11	10.59	10.92	9.25	9.82	6.95	8.30	10.05
	std. dev.	5.33	4.64	5.47	4.89	5.19	5.26	6.18	5.64	5.82	4.23	4.32	6.29
Step 3	mean	11.51	8.06	9.63	11.40	8.84	11.38	10.75	8.63	10.16	7.29	8.54	9.00
	std. dev.	5.70	4.58	5.16	5.34	4.93	5.37	6.13	5.05	–	4.44	4.49	–
Step 4	mean	10.32	6.35	–	11.38	9.05	11.49	11.18	10.34	–	6.16	7.65	–
	std. dev.	5.38	3.73	–	5.79	4.98	5.28	5.69	4.97	–	3.39	4.04	–

Table 4: Result of multiple linear regression of objective function (Step 1).

	Coef.	Std. dev.	t	P-value
Section	–313.2	9.1995	–34.04	0.0000
J_1	4.743	0.2480	19.12	0.0000
J_2	6.260	0.2447	25.58	0.0000
J_3	15.71	0.2487	63.18	0.0000
J_4	–3.793	0.2469	–15.36	0.0000
J_5	5.376	0.2495	21.55	0.0000
J_6	11.67	0.2516	46.38	0.0000
J_7	1.388	0.2462	5.635	0.0000
J_8	1.797	0.2480	7.245	0.0000
J_9	0.522	0.2463	2.119	0.0342
J_{10}	1.680	0.2440	6.884	0.0000
J_{11}	1.736	0.2476	7.013	0.0000
J_{12}	0.314	0.2467	1.274	0.2030

in parentheses is the order of boosting. The categories SMALL and LARGE are converted to real values -1 and 1 , respectively. Therefore, a smaller value indicates large possibility to be classified as SMALL. It is seen from this result that the relation $J_6 \leq 10$, $J_3 \leq 14$, $J_{11} \leq 14$, $J_{10} \leq 17$, or $J_5 \leq 17$ leads to a large chance to select a decent solution. Therefore, the upper bounds are modified as the last column of Table 1, and we carry out another random selection (Step 2). The range of objective function in Step 2 is $[14.12, 397.46]$, which is smaller than Step 1. The histogram of objective function is plotted in Fig. 6. We can confirm from Figs. 4 and 6 that solutions with small objective values are searched in Step 2.

Variation of decent solutions in integer variable is still very large as shown in Table 3. Therefore, there are some redundant variables. We confirmed from linear regression of the objective function that the contribution of J_9 and J_{12} are very small. Therefore, we fix J_{12} at the optimal value of Step 2, and compute J_9 as mean value of J_8 and J_{10} for each randomly generated solution. By carrying out this step called Step 3, the region of objective function is reduced to $[12.08, 375.70]$; however, standard variation of each integer variable is not reduced as shown in Table 3.

Another linear regression is carried out for 2000 solutions generated in Step 3 to find that the contribution of J_3 and J_5 are very large. Therefore, linear regression of J_3 is done for decent solutions to obtain the following approximate formula:

$$J_3 = 43.05 - 0.7235J_1 - 0.9485J_2 + 0.61147J_4 - 0.9136J_5 - 0.7520J_6 - 0.2068J_7 - 0.4143J_8 \quad (5)$$

where the nearest integer is assigned from the right-hand-side value of Eq. (5). The result of random selection (Step 4) using this formula leads to the region $[12.08, 162.57]$ of objective function, which have smaller upper bound than Step 3. The variation of decent solutions is reduced as shown in Table 3 except two variables. The optimal solutions obtained in each step is listed in Table 2. We can see that very different solutions are found in four steps. The stress-strain relation of the optimal solution of Step 4 is plotted in Fig. 7, which shows good agreement with the experimental result.

4. Analysis of cantilever

To verify that the effectiveness of the proposed method in application to structural analysis, elastoplastic cyclic analysis is carried out for the cantilever consisting of rolled wide-flange section H-244 \times 175 \times 7 \times 11. The left end of the cantilever

```

| (1)J6 < 10.5: -0.313
| (1)J6 >= 10.5: 0.923
| | (5)J1 < 8.5: -0.318
| | (5)J1 >= 8.5: 1.912
| | (9)J3 < 6.5: -0.423
| | (9)J3 >= 6.5: 0.787
| | | (10)J7 < 19.5: 1.261
| | | (10)J7 >= 19.5: -0.965
| (2)J3 < 14.5: -0.18
| (2)J3 >= 14.5: 1.234
| | (7)J2 < 5.5: -0.602
| | (7)J2 >= 5.5: 1.519
| (3)J11 < 14.5: -0.168
| (3)J11 >= 14.5: 0.95
| | (8)J2 < 8.5: -0.368
| | (8)J2 >= 8.5: 1.485
| (4)J10 < 17.5: -0.089
| (4)J10 >= 17.5: 1.999
| (6)J5 < 17.5: -0.083
| (6)J5 >= 17.5: 1.826
Legend: -ve = SMALL, +ve = LARGE
Tree size (total number of nodes): 31
Leaves (number of predictor nodes): 21

```

Correctly Classified Instances	1900	95 %
Incorrectly Classified Instances	100	5 %
Kappa statistic	0	
Mean absolute error	0.117	
Root mean squared error	0.218	
Relative absolute error	122.5563 %	
Root relative squared error	100.0348 %	
Total Number of Instances	2000	

```

=== Confusion Matrix ===
  a  b  <-- classified as
0 100 |  a = SMALL
0 1900 |  b = LARGE

```

Figure 5: Output of ADTree.

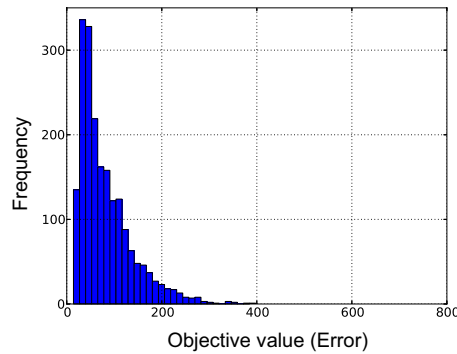


Figure 6: Histogram of objective function $E(\mathbf{J})$ (Step 2).

is clamped, and forced vertical displacement is given at the right end. The (forced) average deflection angle θ of the beam is defined by dividing the tip displacement δ by the beam length $L = 800$ mm. We use ADVENTURECluster [9] for finite element analysis utilizing solid elements.

The web and flange are made of the same material SS400 with different yield stresses. The material is the same as the cyclic test; however, it is made from a different lot, and only monotonic test result is available. Therefore, we carry out another parameter optimization using tabu search to determine the hardening coefficients, whereas the properties of cyclic loading are obtained from the optimal solution of Step 4 in the previous section.

Let \mathbf{a} denote the vector of variables consisting of hardening ratios. The algorithm of TS is summarized as follows:

- S1** Assign an initial seed solution for \mathbf{a} , and initialize the tabu list T to be empty.
- S2** Generate neighborhood solutions of the current seed solution and move to the best feasible solution \mathbf{a}^* among them that is not included in the tabu list T .
- S3** Add \mathbf{a}^* to T . Remove the oldest solution in T if the length of the list exceeds the specified limit.
- S4** Accept \mathbf{a}^* as the next seed solution and go to S2 if the number of steps is less than the specified limit; otherwise, output the best solution and terminate the process.

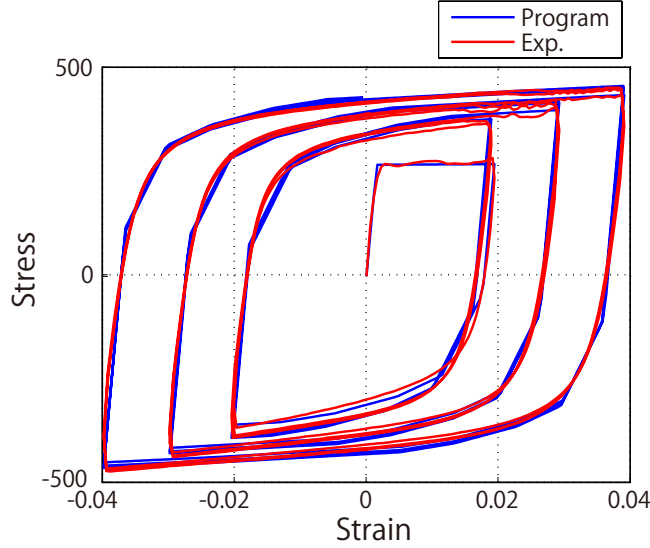


Figure 7: Result of cyclic test (Step 4).

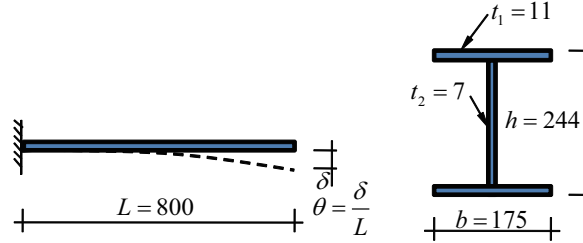


Figure 8: Cantilever with wide-flange section.

The neighborhood solutions are generated using a random number $\tau \in [0, 1]$. Each variable is increased if $\tau \geq 2/3$, decreased if $\tau < 1/3$, and is not modified if $1/3 \leq \tau < 2/3$. The number of neighborhood solutions is 8, and the number of steps is 50. In order to improve accuracy, optimization is carried out from five different initial random seeds, re-sample the variables, as follows, around the best solution.

Yamada *et al.* [6] conducted physical experiments of three different loading patterns RH1, RH2, and RH3 described in terms of deflection angles as shown in Fig. 9: the loading pattern RH1 is symmetric, RH2 gradually deflects in one direction, and RH3 is random.

To investigate the accuracy of the proposed constitutive model for simulation of responses of the cantilever against relatively complex loading patterns, the cantilever is discretized using hexahedral finite elements with linear interpolation function. The flanges and web are divided into three layers. The numbers of elements and nodes in the numerical model are 2700 and 3844, respectively.

For the symmetric loading pattern RH1, the relation between the deflection angle and the bending moment at the fixed end is shown in Fig. 10(a), where the solid and dashed lines respectively stand for experimental and numerical results. For the more complex loading patterns RH2 and RH3, the numerical results together with the experimental results are respectively plotted in Figs. 10(b) and (c). As is seen, the responses evaluated using the proposed model has good accuracy for even these asymmetric loading patterns. It should be noted here that the constitutive parameters are identified using the cyclic and monotonic coupon tests only, and no tuning has been made for the results of cantilever subjected to different loading conditions.

5. Conclusions

An optimization approach has been presented for parameter identification of steel materials using random selection and tabu search. Accuracy of solution can be improved utilizing methods of data mining and statistical analysis. The randomly selected solutions are classified into decent (approximate optimal) solutions and other solutions. The important parameters to find a decent solution are identified by χ^2 -test and correlation analysis. The possibility of searching decent solutions

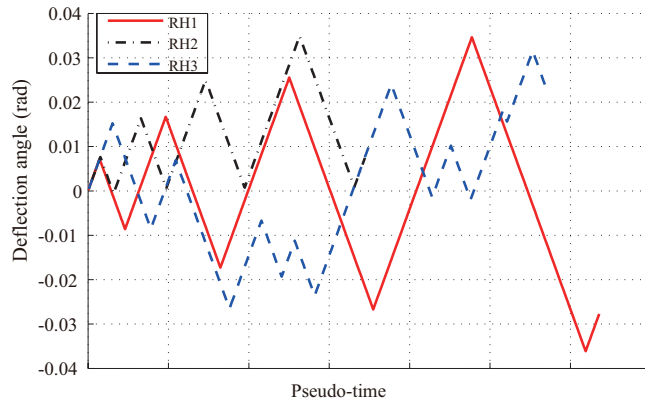


Figure 9: Loading protocols for the cantilever.

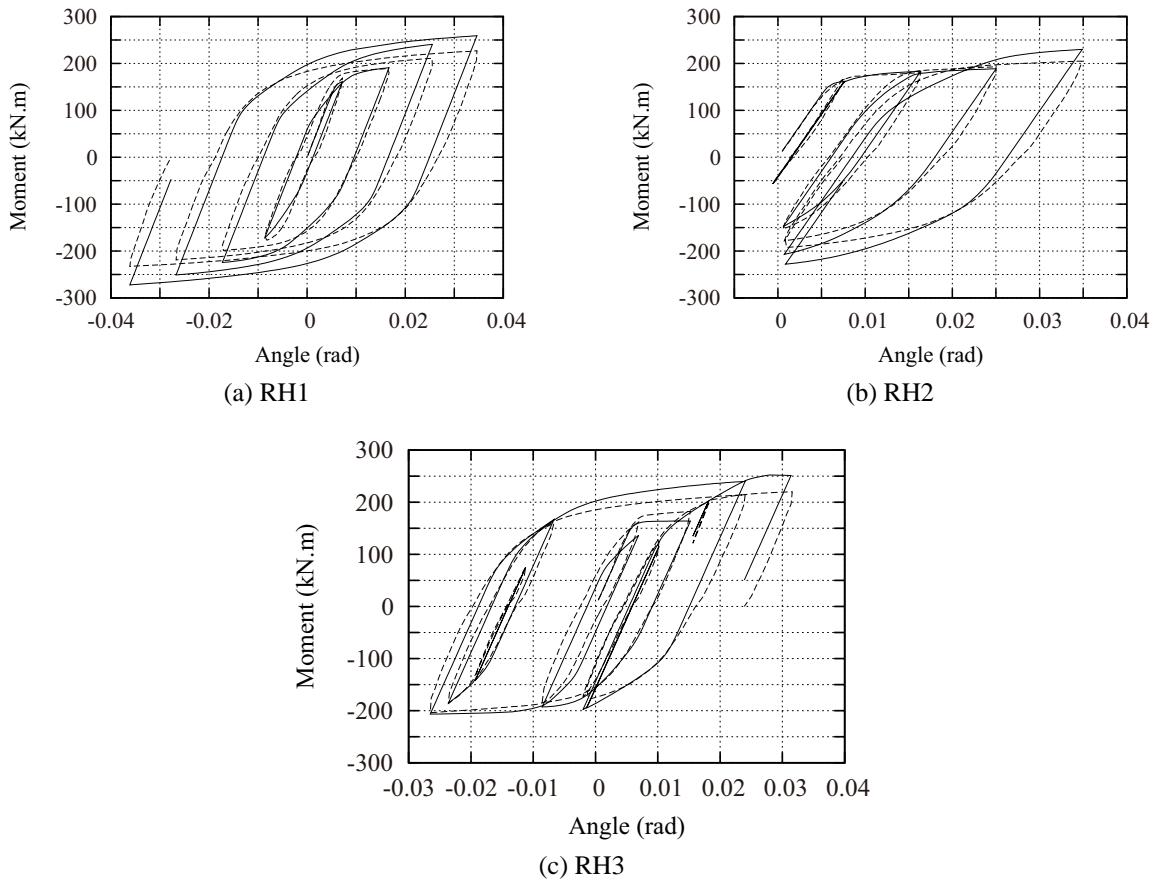


Figure 10: Results of asymmetric loading patterns; solid line: analysis, dotted line: experiment

can be improved using a decision tree to restrict the variables into smaller ranges.

The material parameters of steels such as hardening coefficients and ratio of isotropic hardening can be identified by the proposed method to simulate the result of cyclic material test with good accuracy. It has also been confirmed that the elastoplastic responses of cantilever subjected to cyclic loads can be accurately simulated using the proposed optimization method for parameter identification of piecewise linear combined hardening.

Acknowledgments

This work is partially supported by the Kajima Foundation's Research Grant and a Grant-in-Aid for Scientific Research from JSPS, Japan. The authors would like to thank Prof. Yamada of Tokyo Institute of Technology for providing the authors with valuable experimental data.

References

- [1] J. L. Chaboche, A review of some plasticity and viscoplasticity constitutive theories, *Int. J. Plasticity*, Vol. 24, pp. 1642–1693, 2008.
- [2] F. Yoshida, A constitutive model of cyclic plasticity, *Int. J. Plasticity*, Vol. 16, pp. 359–380, 2000.
- [3] M. Ohsaki, T. Miyamura, M. Kohiyama, J. Y. Zhang, D. Isobe, K. Onda, T. Yamashita, M. Hori, H. Akiba and K. Kajiwara, High-precision FE-analysis of steel frames: Collapse simulation considering composite beam effect, *Proc. EuroSteel 2011, Budapest*, pp. 921–926, 2011.
- [4] F. Glover, Tabu search: Part i, *ORSA J. on Computing*, Vol. 1, pp. 190–206, 1989.
- [5] M. Ohsaki, *Optimization of Finite Dimensional Structures*, CRC Press, 2010.
- [6] S. Yamada, T. Imaeda and K. Okada, Simple hysteresis model of structural steel considering the Bauschinger effect, *J. Struct. Constr. Eng., Architectural Inst. of Japan*, No. 559, pp. 225–232, 2002. (in Japanese)
- [7] M. Hall, E. Frank, G. Holmes, B. Pfahringer, P. Reutemann and I. H. Witten, *The WEKA Data Mining Software: An Update, SIGKDD Explorations*, Volume 11(1), 2009.
- [8] WEKA Ver. 3.6, <http://www.cs.waikato.ac.nz/ml/weka/index.html>
- [9] Alied Engineering, ADVENTURECluster, <http://www.alde.co.jp/>